

1 **A human monoclonal antibody blocking SARS-CoV-2 infection**

2 Running Head: A cross-neutralizing human antibody targeting SARS-CoV and SARS-  
3 CoV-2

4 Chunyan Wang<sup>a,\*\*</sup>, Wentao Li<sup>a,\*\*</sup>, Dubravka Drabek<sup>b,c,\*\*</sup>, Nisreen M.A. Okba<sup>d</sup>, Rien van  
5 Haperen<sup>b,c</sup>, Albert D.M.E. Osterhaus<sup>e</sup>, Frank J.M. van Kuppeveld<sup>a</sup>, Bart L. Haagmans<sup>d</sup>,  
6 Frank Grosveld<sup>b,c,\$</sup> and Berend-Jan Bosch<sup>a,\*,§</sup>

7 Virology Division, Department of Biomolecular Health Sciences, Faculty of Veterinary  
8 Medicine, Utrecht University, Utrecht, the Netherlands<sup>a</sup>; Department of Cell Biology,  
9 Erasmus MC, Rotterdam, the Netherlands<sup>b</sup>; Harbour Antibodies B.V., Rotterdam,  
10 Netherlands<sup>c</sup>; Department of Molecular and Cell Biology, Department of Viroscience,  
11 Erasmus Medical Center, Rotterdam, the Netherlands<sup>d</sup>. University of Veterinary  
12 Medicine, Hannover, Germany<sup>e</sup>

13 \* Address correspondence to Berend-Jan Bosch, [b.j.bosch@uu.nl](mailto:b.j.bosch@uu.nl).

14 \*\* These authors are joint first authors. § These authors are joint senior authors.

15

16 **Abstract**

17 The emergence of the novel human coronavirus SARS-CoV-2 in Wuhan, China has  
18 caused a worldwide epidemic of respiratory disease (COVID-19). Vaccines and  
19 targeted therapeutics for treatment of this disease are currently lacking. Here we report  
20 a human monoclonal antibody that neutralizes SARS-CoV-2 (and SARS-CoV). This  
21 cross-neutralizing antibody targets a communal epitope on these viruses and offers  
22 potential for prevention and treatment of COVID-19.

23

24 **Main text**

25 The severe acute respiratory syndrome coronavirus 2 (SARS-CoV-2) is the etiological  
26 agent of the coronavirus induced disease 19 (COVID-19) that emerged in China late  
27 2019 and causing a worldwide epidemic<sup>1</sup>. As of March 10<sup>th</sup> 2020, over 115,113 cases  
28 have been reported in 109 countries, of which 4,063 (3.5%) succumbed to the  
29 infection<sup>2</sup>. SARS-CoV-2 belongs to the *Sarbecovirus* subgenus (genus  
30 *Betacoronavirus*, family *Coronaviridae*)<sup>3</sup> together with SARS-CoV that emerged in  
31 2002 causing approximately 8000 infections with a lethality of 10%. Both viruses  
32 crossed species barriers from an animal reservoir and can cause a life-threatening  
33 respiratory illness in humans. Presently no approved targeted therapeutics are  
34 available for COVID-19. Monoclonal antibodies targeting vulnerable sites on viral  
35 surface proteins are increasingly recognised as a promising class of drugs against  
36 infectious diseases and have shown therapeutic efficacy for a number of viruses<sup>4, 5</sup>.

37 Coronavirus neutralizing antibodies primarily target the trimeric spike (S) glycoproteins  
38 on the viral surface that mediate entry into host cells. The S protein has two functional  
39 subunits that mediate cell attachment (the S1 subunit, existing of four core domains  
40 S1<sub>A</sub> through S1<sub>D</sub>) and fusion of the viral and cellular membrane (the S2 subunit). Potent  
41 neutralizing antibodies often target the receptor interaction site in S1, disabling  
42 receptor interactions<sup>6-11</sup>. The spike proteins of SARS-CoV-2 (SARS2-S; 1,273  
43 residues, strain Wuhan-Hu-1) and SARS-CoV (SARS-S, 1,255 residues, strain Urbani)  
44 are 77.5% identical by primary amino acid sequence, are structurally very similar<sup>12, 13</sup>  
45 and commonly bind the human angiotensin converting enzyme 2 (ACE2) protein as a  
46 host receptor<sup>1, 14</sup> through their S1<sub>B</sub> domain. Receptor interaction is known to trigger

47 irreversible conformational changes in coronavirus spike proteins enabling membrane  
48 fusion<sup>15</sup>.

49 In order to identify SARS-CoV-2 neutralizing antibodies, ELISA-(cross)reactivity was  
50 assessed of antibody-containing supernatants of a collection of 51 SARS-S  
51 hybridoma's derived from immunized transgenic H2L2 mice that encode chimeric  
52 immunoglobulins with human variable heavy and light chains and constant regions of  
53 rat origin (Suppl.Fig.1). Four of 51 SARS-S hybridoma supernatants displayed ELISA-  
54 cross-reactivity with the SARS2-S1 subunit (S residues 1-681; Suppl.Fig.1), of which  
55 one (47D11) exhibited cross-neutralizing activity of SARS-S and SARS2-S  
56 pseudotyped VSV infection. The chimeric 47D11 H2L2 antibody was reformatted and  
57 recombinantly expressed as a fully human IgG1 isotype antibody for further  
58 characterization.

59 The human 47D11 antibody binds to cells expressing the full-length spike proteins of  
60 SARS-CoV and SARS-CoV-2 (Fig.1a). The 47D11 antibody was found to potently  
61 inhibit infection of VeroE6 cells with SARS-S and SARS2-S pseudotyped VSV with  
62 IC<sub>50</sub> values of 0.06 and 0.08 µg/ml (Fig.1b), respectively. Authentic infection of VeroE6  
63 cells with SARS-CoV and SARS-CoV-2 was neutralized with IC<sub>50</sub> values of 0.19 and  
64 0.57 µg/ml (Fig.1c). Using ELISA 47D11 was shown to target the S1<sub>B</sub> receptor binding  
65 domain (RBD) of SARS-S and SARS2-S. 47D11 bound the S1<sub>B</sub> of both viruses with  
66 similar affinities as shown by the ELISA-based half maximal effective concentration  
67 (EC<sub>50</sub>) values (0.02 and 0.03 µg/ml, respectively; Fig.2a). ELISA-based binding affinity  
68 of 47D11 for the spike ectodomain (S<sub>ecto</sub>) of SARS-CoV was higher relative to that of  
69 SARS-CoV-2 (EC<sub>50</sub> values: 0.018 and 0.15 µg/ml, respectively), despite equimolar  
70 antigen coating (Suppl.Fig.2). Congruent with the ELISA-reactivities, measurement of  
71 binding kinetics of 47D11 by biolayer interferometry showed that 47D11 binds SARS-  
72 S<sub>ecto</sub> with higher affinity (equilibrium dissociation constant [ $K_D$ ]: 0.745 nM) relative to  
73 SARS2-S<sub>ecto</sub> ( $K_D$  10.8 nM) whereas affinity for SARS-S1<sub>B</sub> and SARS2-S1<sub>B</sub> was in a  
74 similar range (16.1 and 9.6 nM, respectively, Suppl.Fig.3). This difference may  
75 originate from differences in epitope accessibility in SARS-S versus SARS2-S, as  
76 domain B can adopt a closed and open conformation in the prefusion spike  
77 homotrimer<sup>12, 13</sup>. Remarkably, binding of 47D11 to SARS-S1<sub>B</sub> and SARS2-S1<sub>B</sub> did not  
78 compete with S1<sub>B</sub> binding to the ACE2 receptor expressed at the cell surface as shown  
79 by flow cytometry (Fig.2b; Suppl.Fig.4) nor with S<sub>ecto</sub> and S1<sub>B</sub> binding to soluble ACE2

80 in solid-phase based assay (Suppl.Fig.5), whereas two SARS-S1 specific antibodies  
81 35F4 and 43C6 that neutralize SARS-S (but not SARS2-S) pseudotyped VSV infection  
82 (Suppl.Fig.6) do block binding of SARS-S<sub>ecto</sub> and SARS-S1<sub>B</sub> to ACE2. Using a trypsin-  
83 triggered cell-cell fusion assay, 47D11 was shown to impair SARS-S and SARS2-S  
84 mediated syncytia formation (Suppl.Fig.7). Our data show that 47D11 neutralizes  
85 SARS-CoV and SARS-CoV-2 through a yet unknown mechanism that is different from  
86 receptor binding interference. Alternative mechanisms of coronavirus neutralization by  
87 RBD-targeting antibodies have been reported including spike inactivation through  
88 antibody-induced destabilization of its prefusion structure<sup>15</sup>, which may also apply for  
89 47D11.

90 The SARS2-S1<sub>B</sub> receptor binding domain (residues 338-506) consists of a core  
91 domain and a receptor binding subdomain (residues 438-498) looping out from the  
92 antiparallel betasheet core domain structure that directly engages the receptor.  
93 Compared to the S1<sub>B</sub> core domain, the protein sequence identity of the S1<sub>B</sub> receptor  
94 interacting subdomain of SARS-S and SARS2-S is substantially lower (46.7% versus  
95 86.3%; Suppl.Fig.8 and Fig.2c). Potent neutralizing antibodies often target this  
96 receptor binding subdomain. However, due to common variations in this subdomain,  
97 these antibodies are often virus-specific and bind and neutralize related viruses  
98 poorly<sup>16, 17</sup>. The cross-reactive nature of 47D11 indicates that the antibody is more  
99 likely to target the conserved core structure of the S1<sub>B</sub> receptor binding domain. S1<sub>B</sub>  
100 binding by 47D11 further away from the receptor binding interface explains its inability  
101 to compromise spike-receptor interaction.

102 In conclusion, this is the first report on a (human) monoclonal antibody that  
103 neutralizes SARS-CoV-2. 47D11 binds a conserved epitope on the spike receptor  
104 binding domain explaining its ability to cross-neutralize SARS-CoV and SARS-CoV-2,  
105 using a mechanism that is independent of receptor binding inhibition. This antibody will  
106 be useful for development of antigen detection tests and serological assays targeting  
107 SARS-CoV-2. Neutralizing antibodies can alter the course of infection in the infected  
108 host supporting virus clearance or protect an uninfected host that is exposed to the  
109 virus<sup>4</sup>. Hence, this antibody offers the potential to prevent and/or treat COVID-19, and  
110 possibly also other future emerging diseases in humans caused by viruses from the  
111 *Sarbecovirus* subgenus.

112

113 **References**

- 114 1. Zhou, P. *et al.* A pneumonia outbreak associated with a new coronavirus of probable  
115 bat origin. *Nature*, 1-4 (2020).
- 116 2. World Health Organization. [https://www.who.int/docs/default-](https://www.who.int/docs/default-source/coronaviruse/situation-reports/20200310-sitrep-50-covid-19.pdf?sfvrsn=55e904fb_2)  
117 [source/coronaviruse/situation-reports/20200310-sitrep-50-covid-](https://www.who.int/docs/default-source/coronaviruse/situation-reports/20200310-sitrep-50-covid-19.pdf?sfvrsn=55e904fb_2)  
118 [19.pdf?sfvrsn=55e904fb\\_2](https://www.who.int/docs/default-source/coronaviruse/situation-reports/20200310-sitrep-50-covid-19.pdf?sfvrsn=55e904fb_2).
- 119 3. Coronaviridae Study Group of the International Committee on Taxonomy of Viruses.  
120 The species Severe acute respiratory syndrome-related coronavirus: classifying 2019-  
121 nCoV and naming it SARS-CoV-2. *Nat. Microbiol.* (2020).
- 122 4. Prabakaran, P. *et al.* Potent human monoclonal antibodies against SARS CoV,  
123 Nipah and Hendra viruses. *Expert opinion on biological therapy* **9**, 355-368 (2009).
- 124 5. Saphire, E. O., Schendel, S. L., Gunn, B. M., Milligan, J. C. & Alter, G. Antibody-  
125 mediated protection against Ebola virus. *Nat. Immunol.* **19**, 1169-1178 (2018).
- 126 6. Reguera, J. *et al.* Structural bases of coronavirus attachment to host aminopeptidase  
127 N and its inhibition by neutralizing antibodies. *PLoS Pathog.* **8**, e1002859 (2012).
- 128 7. Yu, X. *et al.* Structural basis for the neutralization of MERS-CoV by a human  
129 monoclonal antibody MERS-27. *Sci. Rep.* **5**, 13133 (2015).
- 130 8. Prabakaran, P. *et al.* Structure of severe acute respiratory syndrome coronavirus  
131 receptor-binding domain complexed with neutralizing antibody. *J. Biol. Chem.* **281**,  
132 15829-15836 (2006).
- 133 9. Hwang, W. C. *et al.* Structural basis of neutralization by a human anti-severe acute  
134 respiratory syndrome spike protein antibody, 80R. *J. Biol. Chem.* **281**, 34610-34616  
135 (2006).
- 136 10. Rockx, B. *et al.* Structural basis for potent cross-neutralizing human monoclonal  
137 antibody protection against lethal human and zoonotic severe acute respiratory  
138 syndrome coronavirus challenge. *J. Virol.* **82**, 3220-3235 (2008).
- 139 11. Widjaja, I. *et al.* Towards a solution to MERS: protective human monoclonal  
140 antibodies targeting different domains and functions of the MERS-coronavirus spike  
141 glycoprotein. *Emerg. Microbes Infect.* **8**, 516-530 (2019).
- 142 12. Wrapp, D. *et al.* Cryo-EM structure of the 2019-nCoV spike in the prefusion  
143 conformation. *Science* (2020).
- 144 13. Walls, A. C. *et al.* Structure, Function, and Antigenicity of the SARS-CoV-2 Spike  
145 Glycoprotein. *Cell* (2020).
- 146 14. Li, W. *et al.* Angiotensin-converting enzyme 2 is a functional receptor for the SARS  
147 coronavirus. *Nature* **426**, 450-454 (2003).

- 148 15. Walls, A. C. *et al.* Unexpected receptor functional mimicry elucidates activation of  
149 coronavirus fusion. *Cell* **176**, 1026-1039. e15 (2019).
- 150 16. Tian, X. *et al.* Potent binding of 2019 novel coronavirus spike protein by a SARS  
151 coronavirus-specific human monoclonal antibody. *Emerging Microbes & Infections* **9**,  
152 382-385 (2020).
- 153 17. Menachery, V. D. *et al.* A SARS-like cluster of circulating bat coronaviruses shows  
154 potential for human emergence. *Nat. Med.* **21**, 1508 (2015).
- 155 18. Li, F., Li, W., Farzan, M. & Harrison, S. C. Structure of SARS coronavirus spike  
156 receptor-binding domain complexed with receptor. *Science* **309**, 1864-1868 (2005).
- 157 19. Raj, V. S. *et al.* Dipeptidyl peptidase 4 is a functional receptor for the emerging  
158 human coronavirus-EMC. *Nature* **495**, 251-254 (2013).
- 159 20. Okba, N. M. A. *et al.* Sensitive and Specific Detection of Low-Level Antibody  
160 Responses in Mild Middle East Respiratory Syndrome Coronavirus Infections. *Emerg.*  
161 *Infect. Dis.* **25**, 1868-1877 (2019).

162 **Figure Legends**

163 **Fig.1 47D11 neutralizes SARS-CoV and SARS-CoV-2.** a) Binding of 47D11 to HEK-  
164 293T cells expressing GFP-tagged spike proteins of SARS-CoV and SARS-CoV-2  
165 detected by immunofluorescence assay. The human mAb 7.7G6 targeting the MERS-  
166 CoV S<sub>1B</sub> spike domain was taken along as a negative control, cell nuclei in the overlay  
167 images are visualized with DAPI. b) Antibody-mediated neutralization of infection of  
168 luciferase-encoding VSV particles pseudotyped with spike proteins of SARS-CoV and  
169 SARS-CoV-2. Pseudotyped VSV particles pre-incubated with antibodies at indicated  
170 concentrations (see methods) were used to infect VeroE6 cells and luciferase activities  
171 in cell lysates were determined at 24 h post transduction to calculate infection (%)  
172 relative to non-antibody-treated controls. The average  $\pm$  SD from at least two  
173 independent experiments performed is shown. Iso-CTRL: irrelevant isotype  
174 monoclonal antibody. c) Antibody-mediated neutralization of SARS-CoV and SARS-  
175 CoV-2 infection on VeroE6 cells. The experiment was performed with triplicate  
176 samples, the average  $\pm$  SD is shown.

177

178 **Fig.2 The neutralizing 47D11 monoclonal antibody binds the receptor binding**  
179 **domain of SARS-CoV and SARS-CoV-2 spike proteins without eliminating**  
180 **S<sub>1B</sub>/ACE2 receptor interaction.** a) ELISA binding curves of 47D11 to S<sub>ecto</sub> (upper  
181 panel) or S<sub>1A</sub> and S<sub>1B</sub> (RBD) (lower panel) of SARS-S and SARS2-S coated at  
182 equimolar concentrations. The average  $\pm$  SD from at least two independent  
183 experiments performed is shown. b) Interference of antibodies with binding of the S-  
184 S<sub>1B</sub> of SARS-CoV and SARS-CoV-2 to cell surface ACE2-GFP analysed by flow  
185 cytometry. Prior to cell binding, S<sub>1B</sub> was mixed with mAb (mAbs 47D11, 35F4, 43C6,  
186 7.7G6, in H2L2 format) with indicated specificity in a mAb:S<sub>1B</sub> molar ratio of 8:1 (see  
187 Suppl.Fig.4 for an extensive analysis using different mAb:S<sub>1B</sub> molar ratio's). Cells are  
188 analysed for (ACE2-)GFP expression (x-axis) and S<sub>1B</sub> binding (y-axis). Percentages  
189 of cells that scored negative, single positive, or double positive are shown in each  
190 quadrant. c) Divergence in surface residues in S<sub>1B</sub> of SARS-CoV and SARS-CoV-2.  
191 Upper panel: Structure of the SARS-CoV spike protein S<sub>1B</sub> RBD in complex with  
192 human ACE2 receptor (PDB: 2AJF)<sup>18</sup>. ACE2 (wheat color) is visualized in ribbon  
193 presentation. The S<sub>1B</sub> core domain (blue) and subdomain (orange) are displayed in  
194 surface presentation using PyMOL, and are visualized with the same colors in the



195 linear diagram of the spike protein above, with positions of the S1 and S2 subunits, the  
196 S ectodomain ( $S_{\text{ecto}}$ ), the S1 domains  $S1_{\text{A-D}}$  and the transmembrane domain (TM)  
197 indicated. Lower panel: Similar as panel above with surface residues on  $S1_{\text{B}}$  of SARS-  
198 CoV that are at variance with SARS-CoV-2 colored in white.

199

## 200 **Acknowledgements**

201 We thank dr. Yoshiharu Matsuura (Osaka University, Japan) for the provision of the  
202 luciferase-encoding VSV-G pseudotyped VSV $\Delta$ G-luc virus, and Yongle Yang, Michael  
203 van der Reijden and Rick Janssens for technical support. We thank Christian Drosten  
204 (Charité Universitätsmedizin Berlin, Germany) for provision of the SARS-CoV-2 virus.  
205 This study was done within the framework of National Centre for One Health (NCOH)  
206 and the Innovative Medicines Initiative (IMI) Zoonotic Anticipation and Preparedness  
207 Initiative [ZAPI project; grant agreement no. 115760]. The mice used in this study were  
208 provided by Harbour Antibodies BV, a daughter company of Harbour Biomed  
209 (<http://www.harbourbiomed.com>). C. Wang was supported by a grant from the Chinese  
210 Scholarship Council (file number CSC201708620178).

211

## 212 **Author Contributions**

213 B.J.B. designed and coordinated the study. C.W., W.L., N.M.A.O., R.v.H. and D.D  
214 conducted the experiments. D.D., B.L.H. and B.J.B. supervised part of the  
215 experiments. All authors contributed to the interpretations and conclusions presented.  
216 B.J.B. wrote the manuscript, B.L.H., F.J.M.K., A.D.M.E.O. and F.G. participated in  
217 editing the manuscript.

218

## 219 **Materials and Methods**

220

221 **Expression and purification of coronavirus spike proteins.** Coronavirus spike  
222 ectodomains ( $S_{\text{ecto}}$ ) of SARS-CoV (residues 1–1,182; strain CUHK-W1; GenBank:  
223 AAP13567.1) and SARS-CoV-2 (residues 1–1,213; strain Wuhan-Hu-1; GenBank:  
224 QHD43416.1) were expressed transiently in HEK-293T cells with a C-terminal



225 trimerization motif and Strep-tag using the pCAGGS expression plasmid. Similarly,  
226 pCAGGS expression vectors encoding S1 or its subdomains of SARS-CoV (S1,  
227 residues 1-676; S1<sub>A</sub>, residues 1-302; S1<sub>B</sub>, residues, 325-533), and SARS-CoV-2 (S1,  
228 residues 1-682; S1<sub>A</sub>, residues 1-294; S1<sub>B</sub>, residues 329-538) C-terminally tagged with  
229 Fc domain of human or mouse IgG or Strep-tag were generated as described before<sup>19</sup>.  
230 Recombinant proteins were expressed transiently in HEK-293T cells and affinity  
231 purified from the culture supernatant by protein-A sepharose beads (GE Healthcare)  
232 or streptactin beads (IBA) purification. Purity and integrity of all purified recombinant  
233 proteins was checked by coomassie stained SDS-PAGE.

234 **Generation of H2L2 mAbs.** H2L2 mice were sequentially immunized in two weeks  
235 intervals with purified S<sub>ecto</sub> of different CoVs in the following order: HCoV-OC43, SARS-  
236 CoV, MERS-CoV, HCoV-OC43, SARS-CoV and MERS-CoV. Antigens were injected  
237 at 20-25 µg/mouse using Stimune Adjuvant (Prionics) freshly prepared according to  
238 the manufacturer instruction for first injection, while boosting was done using Ribi  
239 (Sigma) adjuvant. Injections were done subcutaneously into the left and right groin  
240 each (50 µl) and 100 µl intraperitoneally. Four days after the last injection, spleen and  
241 lymph nodes are harvested, and hybridomas made by standard method using SP 2/0  
242 myeloma cell line (ATCC#CRL-1581) as a fusion partner. Hybridomas were screened  
243 in antigen-specific ELISA and those selected for further development, subcloned and  
244 produced on a small scale (100 ml of medium). For this purpose, hybridomas are  
245 cultured in serum- and protein-free medium for hybridoma culturing (PFHM-II (1X),  
246 Gibco) with addition of non-essential amino acids 100X NEAA, Biowhittaker Lonza,  
247 Cat BE13-114E). H2L2 antibodies were purified from hybridoma culture supernatants  
248 using Protein-A affinity chromatography. Purified antibodies were stored at 4°C until  
249 use.

250 **Production of human monoclonal antibody 47D11.** For recombinant human mAb  
251 production, the cDNA's encoding the 47D11 H2L2 mAb variable regions of the heavy  
252 and light chains were cloned into expression plasmids containing the human IgG1  
253 heavy chain and Ig kappa light chain constant regions, respectively (InvivoGen). Both  
254 plasmids contain the interleukin-2 signal sequence to enable efficient secretion of  
255 recombinant antibodies. Recombinant human 47D11 mAb and previously described  
256 Isotype-control (anti-Streptag mAb) or 7.7G6 mAb were produced in HEK-293T cells  
257 following transfection with pairs of the IgG1 heavy and light chain expression plasmids

258 according to protocols from InvivoGen. Human antibodies were purified from cell  
259 culture supernatants using Protein-A affinity chromatography. Purified antibodies were  
260 stored at 4°C until use.

261 **Immunofluorescence microscopy.** Antibody binding to cell surface spike proteins of  
262 SARS-CoV, SARS-CoV-2 and MERS-CoV was measured by immunofluorescence  
263 microscopy. HEK-293T cells seeded on glass slides were transfected with plasmids  
264 encoding SARS-S, SARS2-S or MERS-S - C-terminally fused to the green  
265 fluorescence protein (GFP) - using Lipofectamine 2000 (Invitrogen). Two days post  
266 transfection, cells were fixed by incubation with 2% paraformaldehyde in PBS for 20  
267 min at room temperature and stained for nuclei with 4,6-diamidino-2-phenylindole  
268 (DAPI). Cells were subsequently incubated with mAbs at a concentration of 10 µg/ml  
269 for 1 h at room temperature, followed by incubation with Alexa Fluor 594 conjugated  
270 goat anti-human IgG antibodies (Invitrogen, Thermo Fisher Scientific) for 45 min at  
271 room temperature. The fluorescence images were recorded using a Leica Spell  
272 confocal microscope.

273 **Flow cytometry-based receptor binding inhibition assay.** Antibody interference of  
274 S1<sub>B</sub> binding to human ACE2 receptor on the cell surface was measured by flow  
275 cytometry. HEK-293T cells were seeded at a density of 2.5×10<sup>5</sup> cells per ml in a T75  
276 flask. After reaching 70~80% confluency, cells were transfected with an expression  
277 plasmid encoding human ACE2 - C-terminally fused to the GFP - using Lipofectamine  
278 2000 (Invitrogen). Two days post transfection, cells were dissociated by cell  
279 dissociation solution (Sigma-aldrich, Merck KGaA; cat. no. C5914). 2.5 µg/ml of human  
280 Fc tagged SARS-S1<sub>B</sub> and SARS2-S1<sub>B</sub> was preincubated with mAb at the indicated  
281 mAb:S1<sub>B</sub> molar ratios for 1 hour on ice and subjected to flow cytometry. Single cell  
282 suspensions in FACS buffer were centrifuged at 400×g for 10 min. Cells were  
283 subsequently incubated with S1<sub>B</sub> and mAb mixture for 1 h on ice, followed by  
284 incubation with Alexa Fluor 594 conjugated goat anti-human IgG antibodies  
285 (Invitrogen, Thermo Fisher Scientific) for 45 min at room temperature. Cells were  
286 subjected to flow cytometric analysis with a CytoFLEX Flow Cytometer (Beckman  
287 Coulter). The results were analysed by FlowJo (version 10).

288 **Pseudotyped virus neutralization assay.** Production of VSV pseudotyped with  
289 SARS-S and SARS2-S was performed as described previously with some  
290 adaptations<sup>11</sup>. Briefly, HEK-293T cells were transfected with pCAGGS expression

291 vectors encoding SARS-S or SARS2-S carrying a 28- or 18-a.a. cytoplasmic tail  
292 truncation, respectively. One day post transfection, cells were infected with the VSV-  
293 G pseudotyped VSV $\Delta$ G bearing the firefly (*Photinus pyralis*) luciferase reporter gene.  
294 Twenty-four hours later, supernatants containing SARS-S/SARS2-S pseudotyped  
295 VSV particles were harvested and titrated on African green monkey kidney VeroE6  
296 cells. In the virus neutralization assay, mAbs were serially diluted at two times the  
297 desired final concentration in DMEM supplemented with 1% fetal calf serum (Bodinco),  
298 100 U/ml Penicillin and 100  $\mu$ g/ml Streptomycin. Diluted mAbs were incubated with an  
299 equal volume of pseudotyped VSV particles for 1 hour at room temperature, inoculated  
300 on confluent VeroE6 monolayers in 96-well plated, and further incubated at 37°C for  
301 24 hours. Luciferase activity was measured on a Berthold Centro LB 960 plate  
302 luminometer using D-luciferin as a substrate (Promega). The percentage of infectivity  
303 was calculated as ratio of luciferase readout in the presence of mAbs normalized to  
304 luciferase readout in the absence of mAb. The half maximal inhibitory concentrations  
305 (IC<sub>50</sub>) were determined using 4-parameter logistic regression (GraphPad Prism version  
306 8).

307 **Virus neutralization assay.** Neutralization of authentic SARS-CoV and SARS-CoV-2  
308 was performed using a plaque reduction neutralization test (PRNT) as described  
309 earlier, with some modifications<sup>20</sup>. In brief, mAbs were two-fold serially diluted and  
310 mixed with SARS-CoV or SARS-CoV-2 for 1 hour. The mixture was then added to  
311 VeroE6 cells and incubated for 1 hr, after which the cells were washed and further  
312 incubated in medium for 8 hrs. The cells were then fixed and stained using a rabbit  
313 anti-SARS-CoV serum (Sino Biological) and a secondary peroxidase-labelled goat  
314 anti-rabbit IgG (Dako). The signal was developed using a precipitate forming TMB  
315 substrate (True Blue, KPL) and the number of infected cells per well were counted  
316 using the ImmunoSpot® Image analyzer (CTL Europe GmbH). The half maximal  
317 inhibitory concentrations (IC<sub>50</sub>) were determined using 4-parameter logistic regression  
318 (GraphPad Prism version 8).

319 **ELISA analysis of antibody binding to CoV spike antigens.** NUNC Maxisorp plates  
320 (Thermo Scientific) were coated with equimolar antigen amounts at 4°C overnight.  
321 Plates were washed three times with Phosphate Saline Buffer (PBS) containing 0.05%  
322 Tween-20 and blocked with 3% Bovine Serum Albumin (BSA) in PBS containing 0.1%  
323 Tween-20 at room temperature for 2 hours. Four-folds serial dilutions of mAbs starting

324 at 10 µg/ml (diluted in blocking buffer) were added and plates were incubated for 1  
325 hour at room temperature. Plates were washed three times and incubated with HRP-  
326 conjugated goat anti-human secondary antibody (ITK Southern Biotech) diluted 1:2000  
327 in blocking buffer for 1 hour at room temperature. An HRP-conjugated anti-StrepMAb  
328 (IBA, Cat.no: 2-1509-001) antibody was used to corroborate equimolar coating of the  
329 Strep-tagged spike antigens. HRP activity was measured at 450 nanometer using  
330 tetramethylbenzidine substrate (BioFX) and an ELISA plate reader (EL-808, Biotek).  
331 Half-maximum effective concentration (EC<sub>50</sub>) binding values were calculated by non-  
332 linear regression analysis on the binding curves using GraphPad Prism (version 8).

Fig.1

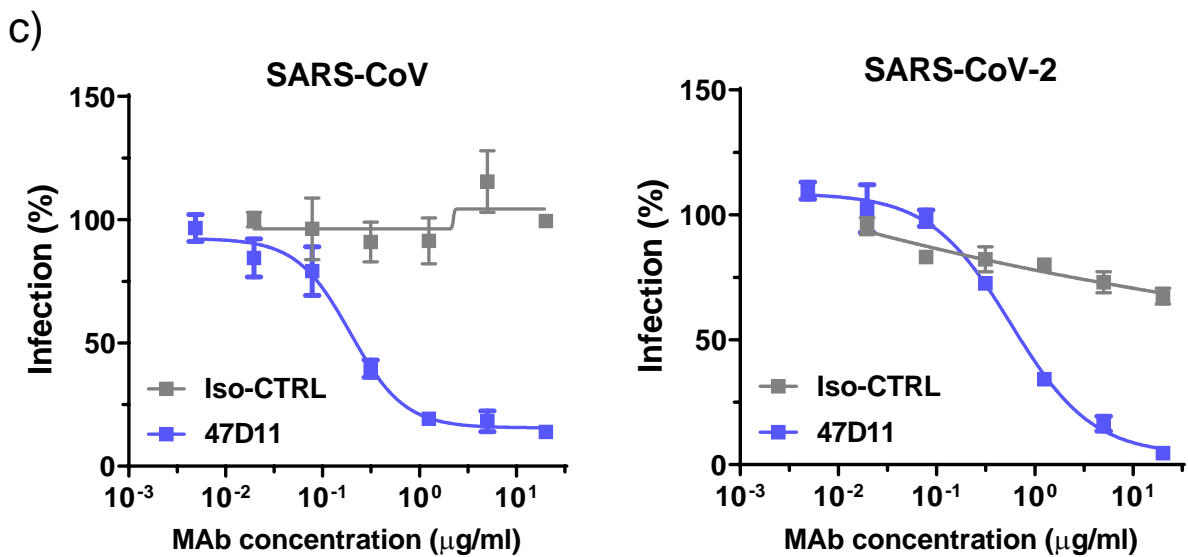
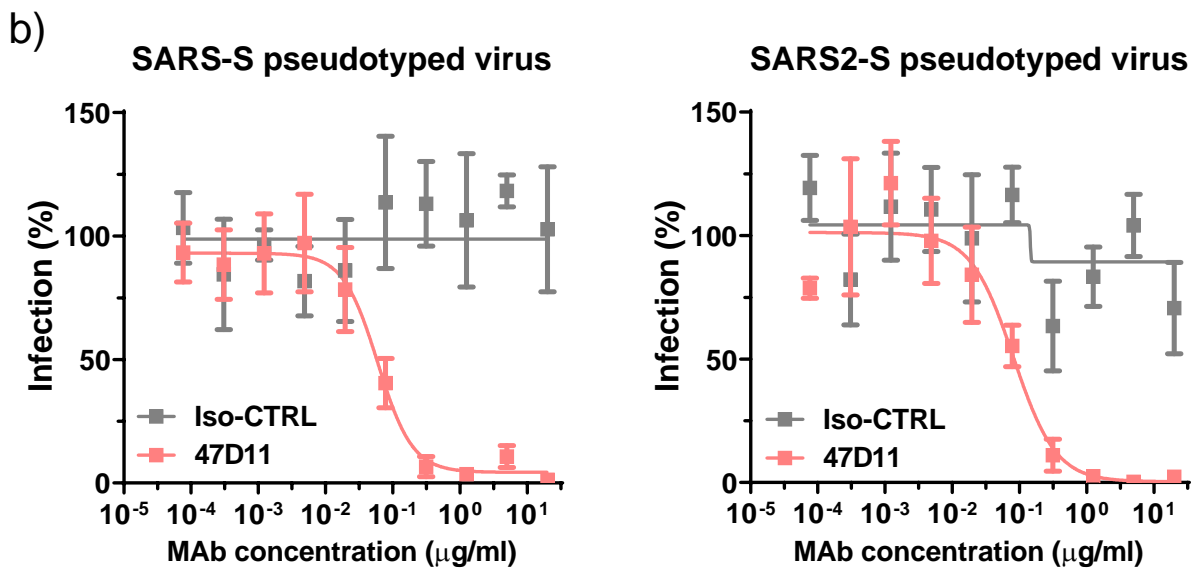
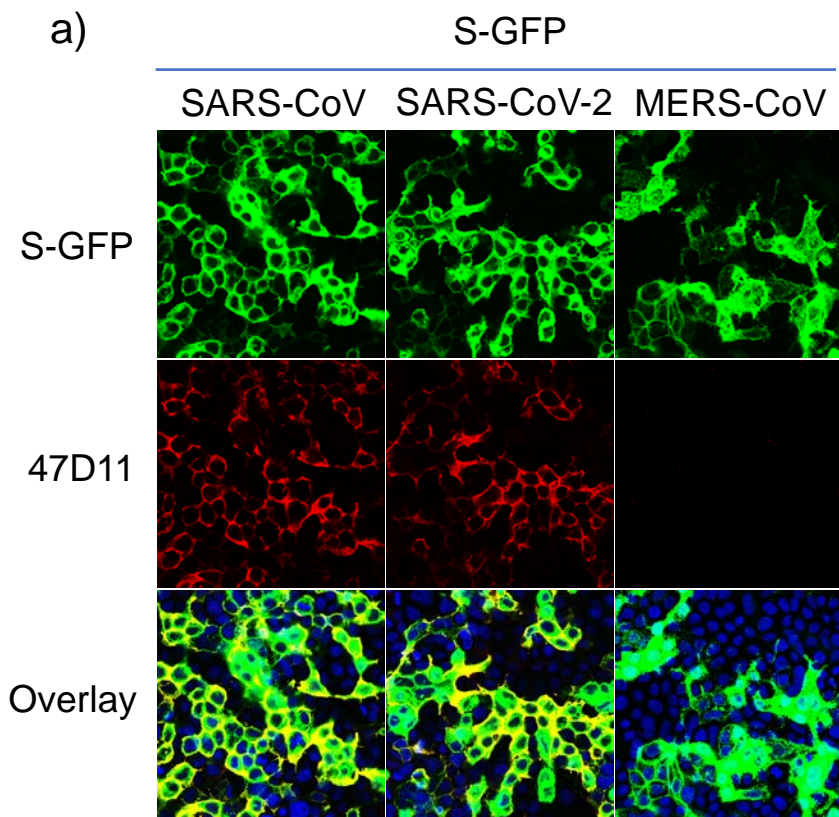
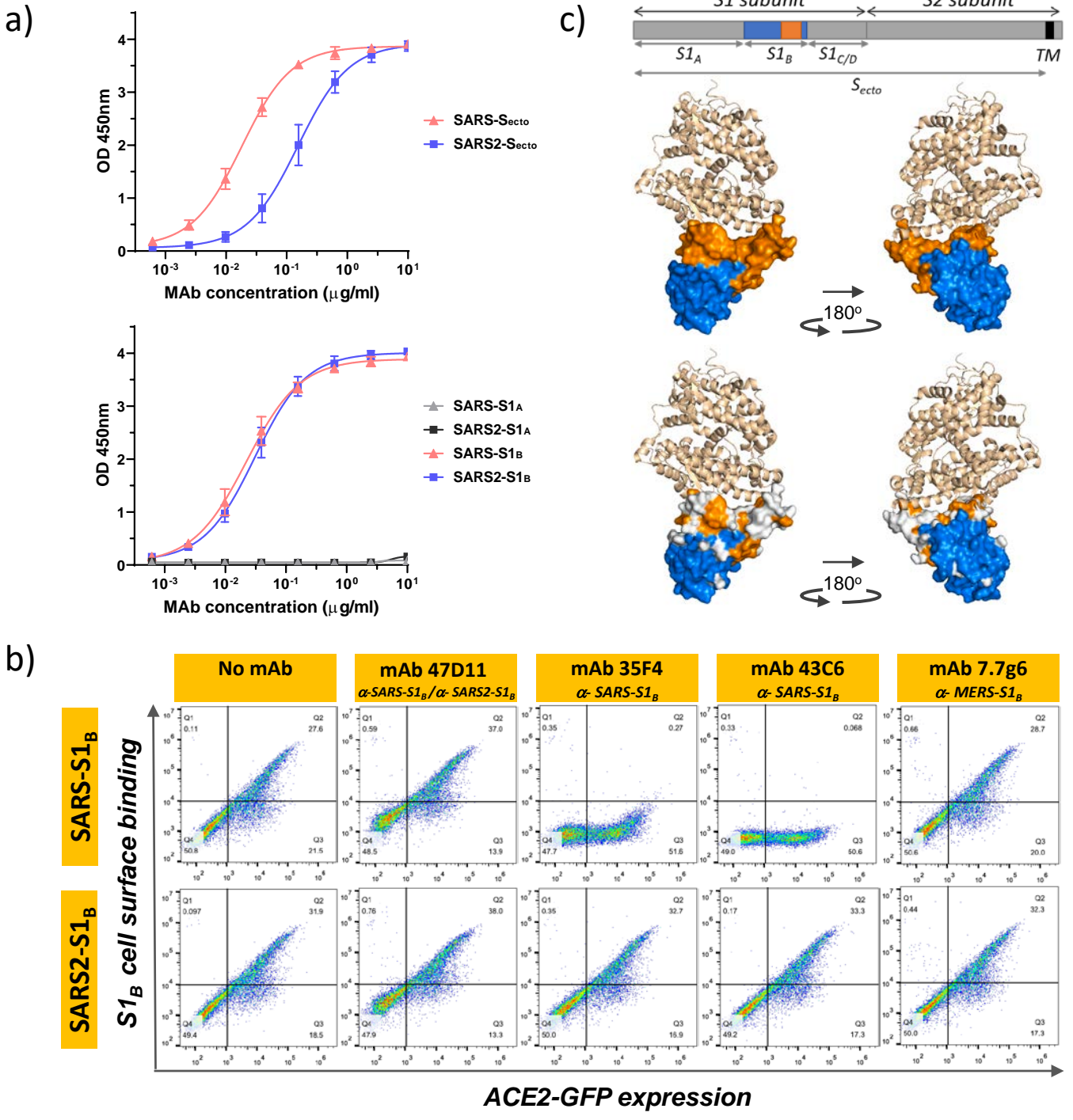


Fig.2





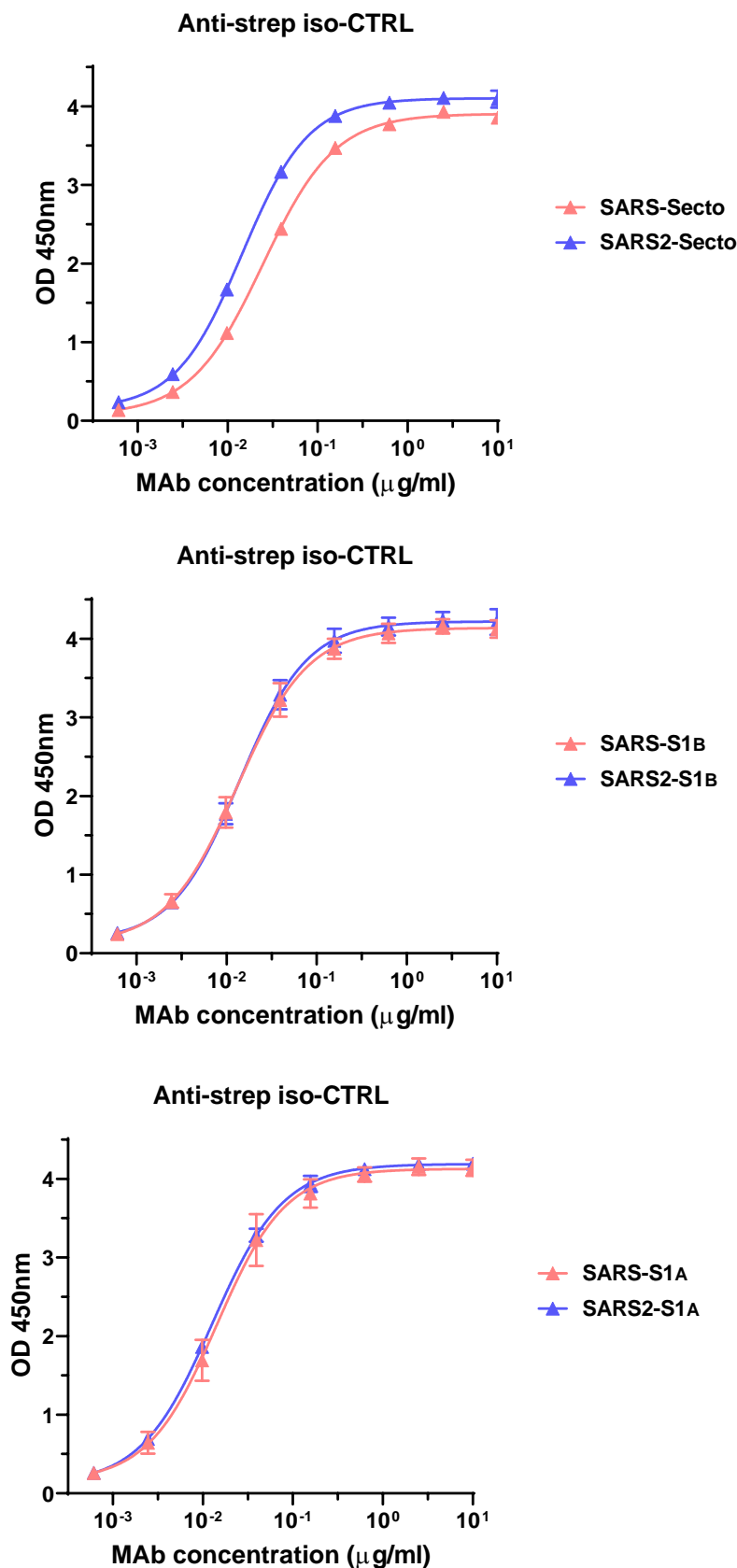
Hybridoma	SARS-S <sub>ecto</sub>	SARS-S1	SARS-S1 <sub>A</sub>	SARS2-S1
44B3	2,5	2,7	3,3	0,1
45E10	3,0	0,8	1,7	0,0
46F11	2,4	2,7	3,3	0,0
39F9	2,9	3,3	3,5	0,0
41A7	2,6	1,0	1,9	0,0
28 E3	2,4	2,3	3,2	0,0
34C10	1,3	1,0	1,9	0,0
16C10	2,4	0,6	1,7	0,1
14B1	2,6	2,9	3,3	0,1
30B1	0,6	0,5	1,1	0,0
28G10	1,0	1,3	2,6	0,0
28F6	2,4	2,9	3,0	0,0
40H10	1,2	0,7	1,9	0,0
39A4	1,7	1,5	2,8	0,0
37G1	1,3	0,9	1,7	0,0
44E11	2,8	3,3	3,5	0,1
19C1	1,9	0,4	1,2	0,1
58D2	2,6	2,8	3,4	0,1
14C1	2,8	1,2	2,6	0,0
45H1	2,3	3,1	3,6	0,0
24F5	3,3	3,4	3,6	0,0
52D9	1,5	1,6	2,3	1,3
45E6	2,4	2,6	3,3	0,0
47D11	3,4	3,0	0,0	1,5
47G10	2,6	2,8	0,1	0,0
48G1	3,3	3,4	0,1	0,0
49F1	1,8	2,0	0,0	1,3
43C6	3,1	3,4	0,1	0,1
22E10	3,2	3,4	0,1	0,0
28D11	2,7	3,1	0,1	0,0
28H3	2,8	1,8	0,0	0,0
25E7	3,1	3,3	0,1	0,1
22E8	1,2	1,2	0,1	0,0
35F4	3,2	3,6	0,1	0,0
43G5	3,2	3,3	0,1	0,1
47F8	1,4	1,4	0,0	0,0
43B4	3,2	3,3	0,1	0,0
49B10	1,1	0,6	0,0	0,2
51C11	1,9	1,9	0,0	0,0
36F6	1,7	2,7	0,1	0,3
65H8	3,2	3,3	0,1	0,1
65H9	1,6	1,7	0,1	2,5
48D5	3,3	3,5	0,1	0,0
35E2	2,5	3,3	0,2	0,0
44G3	2,4	2,8	0,1	0,0
9H9	1,8	0,1	0,0	0,1
25C3	3,0	0,1	0,1	0,1
29E6	1,1	0,1	0,1	0,0
43F11	2,8	0,1	0,1	0,0
47C4	1,5	0,0	0,1	0,0
13F11	3,0	0,0	0,0	0,0

ELISA reactivity hybr. sups	# hybr sups
anti-SARS-S1 <sub>A</sub>	23
anti-SARS-S1 (but not binding S1 <sub>A</sub> )	22
anti-SARS-S <sub>ecto</sub> (but not binding S1)	6
Total	51

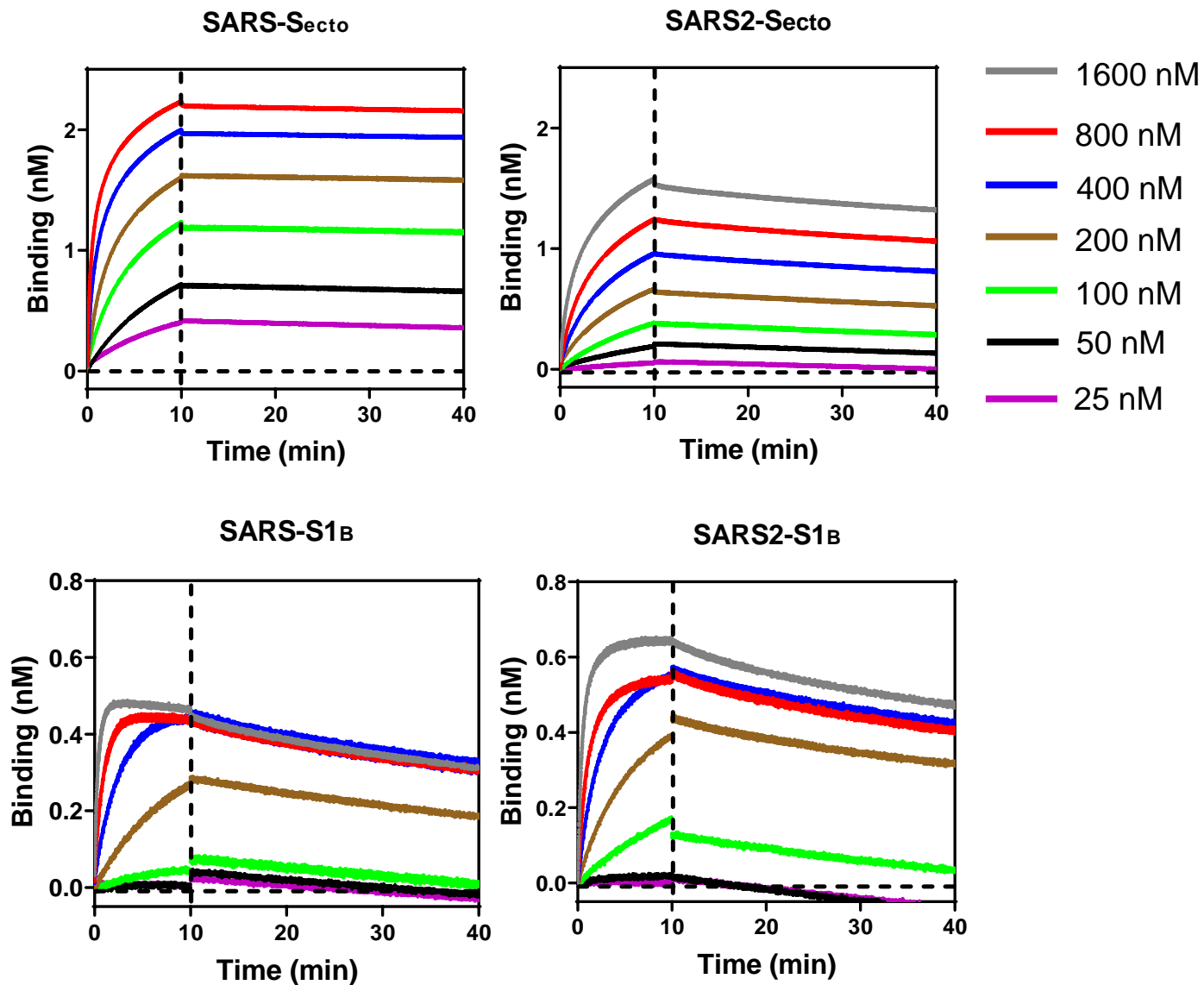
**Suppl. Fig.1. ELISA cross-reactivity of antibody-containing supernatants of SARS-S H2L2 hybridomas towards SARS2-S1.** SARS-S targeting hybridomas were developed by conventional hybridoma technology from immunized H2L2 transgenic mice (Harbour Biomed), as described before<sup>1</sup>. These mice - carrying genes encoding the heavy and light chain human immunoglobulin repertoire - were sequentially immunized with 2-week intervals with trimeric spike protein ectodomains (S<sub>ecto</sub>) of three human coronaviruses from the betacoronavirus genus in the following order: 1. HCoV-OC43-S<sub>ecto</sub>, 2. SARS-CoV-S<sub>ecto</sub>, 3. MERS-CoV-S<sub>ecto</sub>, 4. HCoV-OC43-S<sub>ecto</sub>, 5. SARS-CoV-S<sub>ecto</sub>, 6. MERS-CoV-S<sub>ecto</sub>. Four days after the last immunization, splenocytes and lymph node lymphocytes were harvested and hybridomas were generated. Antibodies in the cell supernatants were tested for ELISA-reactivity against SARS-S<sub>ecto</sub>, SARS-S1, SARS-S1<sub>A</sub> and SARS2-S1. Of the 51 hybridoma supernatants that reacted with SARS-S<sub>ecto</sub> only, 23 reacted with SARS-S1<sub>A</sub>, 22 with SARS-S1 but not SARS-S1<sub>A</sub>, 6 with SARS-S<sub>ecto</sub> but not SARS-S1. Four of the 51 SARS-S<sub>ecto</sub> hybridoma supernatants reacted with SARS2-S1 (see column on the right). The table displays ELISA-signal intensities (OD<sub>450nm</sub> values) of hybridoma supernatants for the different antigens.

1) Widjaja, I. et al. Towards a solution to MERS: protective human monoclonal antibodies targeting different domains and functions of the MERS-coronavirus spike glycoprotein. *Emerg. Microbes Infect.* 8, 516-530 (2019).





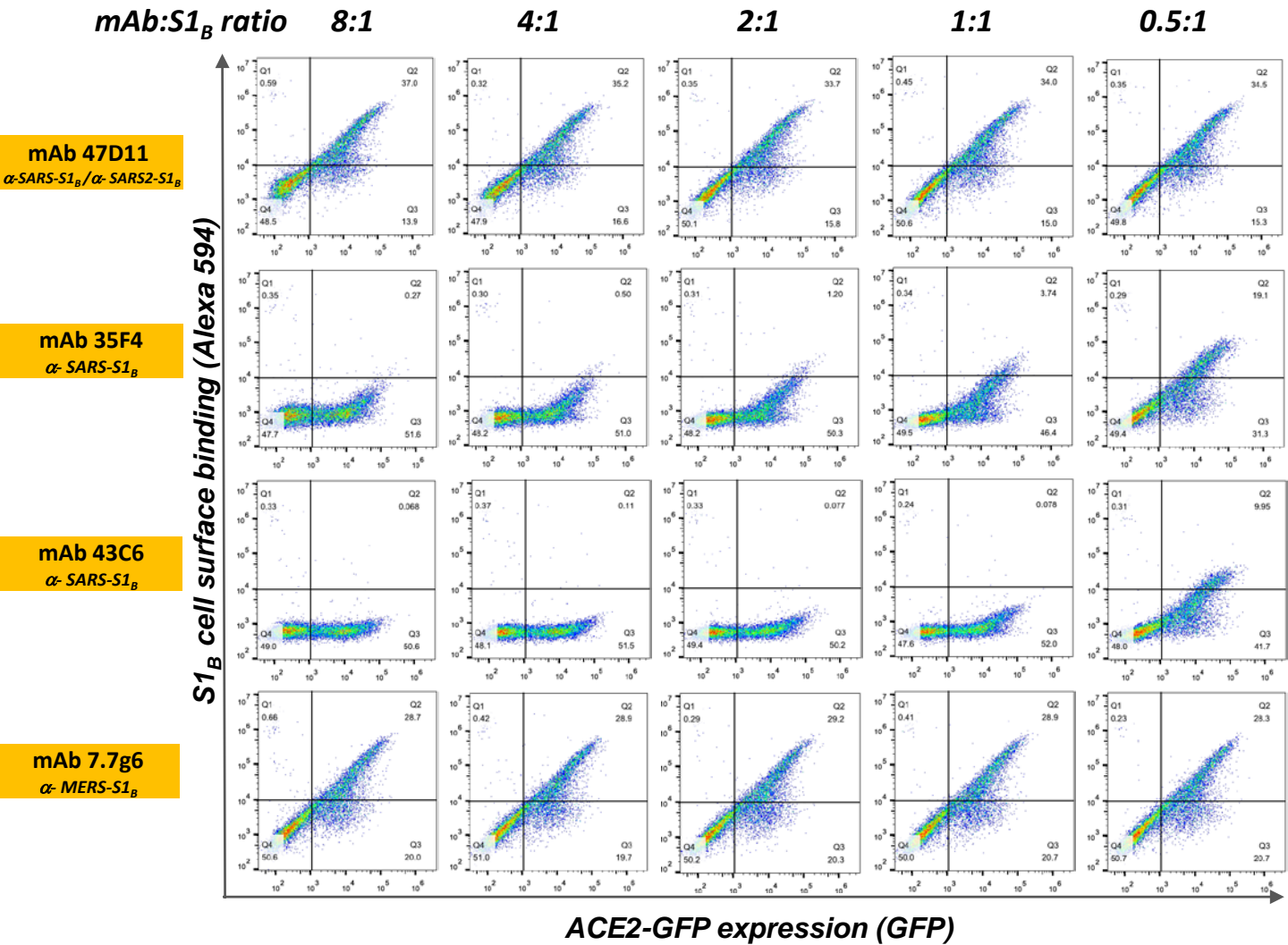
**Suppl. Fig.2.** ELISA binding curve of the anti-StrepMAb (IBA) antibody to Strep-tagged spike antigens to corroborate equimolar ELISA plate coating of SARS-S<sub>ecto</sub> / SARS2-S<sub>ecto</sub> (upper panel), SARS-S1<sub>B</sub> / SARS2-S1<sub>B</sub> (middle panel) and SARS-S1<sub>A</sub> / SARS2-S1<sub>A</sub> (lower panel) antigens used in Fig.2a.



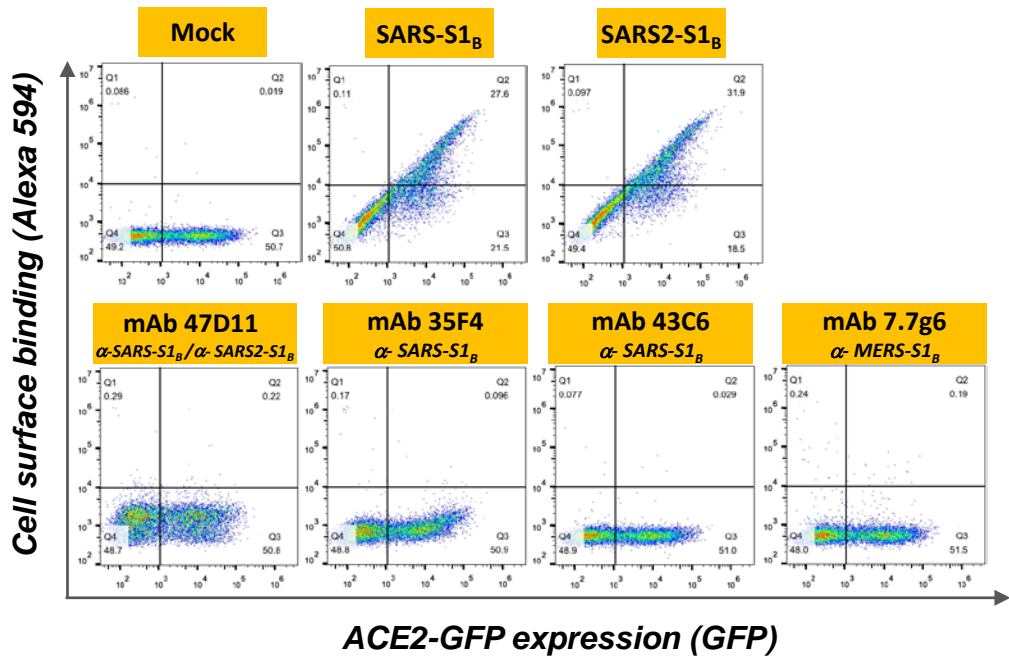
Spike protein	$K_D$ (nM)	$K_{on}$ ( $M^{-1}sec^{-1}$ )	$K_{off}$ ( $sec^{-1}$ )
SARS-S <sub>ecto</sub>	0.745 ( $\pm$ 0.532)	$3.75$ ( $\pm$ 1.27) $\times 10^4$	$3.42$ ( $\pm$ 3.34) $\times 10^{-5}$
SARS2-S <sub>ecto</sub>	10.8 ( $\pm$ 2.46)	$9.77$ ( $\pm$ 4.09) $\times 10^3$	$9.85$ ( $\pm$ 3.61) $\times 10^{-5}$
SARS-S <sub>1B</sub>	16.1 ( $\pm$ 13.3)	$2.00$ ( $\pm$ 0.961) $\times 10^4$	$2.10$ ( $\pm$ 0.239) $\times 10^{-4}$
SARS2-S <sub>1B</sub>	9.56 ( $\pm$ 2.68)	$1.51$ ( $\pm$ 0.285) $\times 10^4$	$1.37$ ( $\pm$ 0.0728) $\times 10^{-4}$

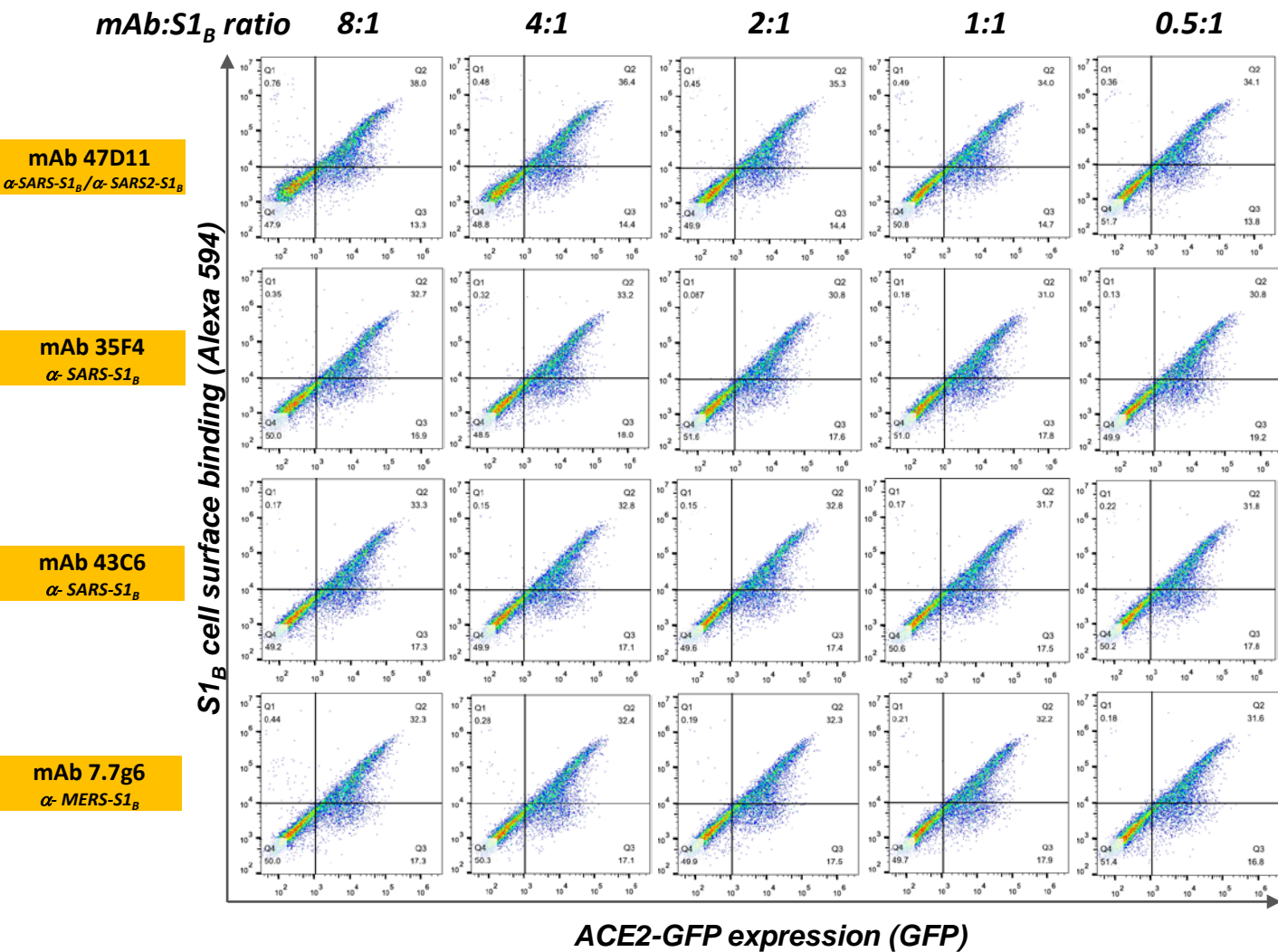
**Suppl. Fig.3. Binding kinetics of 47D11 to the S ectodomain and S1<sub>B</sub> of SARS-CoV and SARS-CoV-2.** Binding kinetics of 47D11 to immobilized recombinant SARS-S<sub>ecto</sub>, SARS2-S<sub>ecto</sub>, SARS-S1<sub>B</sub> and SARS2-S1<sub>B</sub> was measured using biolayer interferometry at 25°C, as described previously<sup>21</sup>. Kinetic binding assay was performed by loading 47D11 mAb at optimal concentration (42 nM) on anti-human Fc biosensor for 10 mins. Antigen association step was performed by incubating the sensor with a range of concentrations of the recombinant spike ectodomain (1600-800-400-200-100-50-25 nM) for 10 min, followed by a dissociation step in PBS for 60 min. The kinetics constants were calculated using 1:1 Langmuir binding model on Fortebio Data Analysis 7.0 software.

### SARS-S1<sub>B</sub> – ACE2 receptor binding

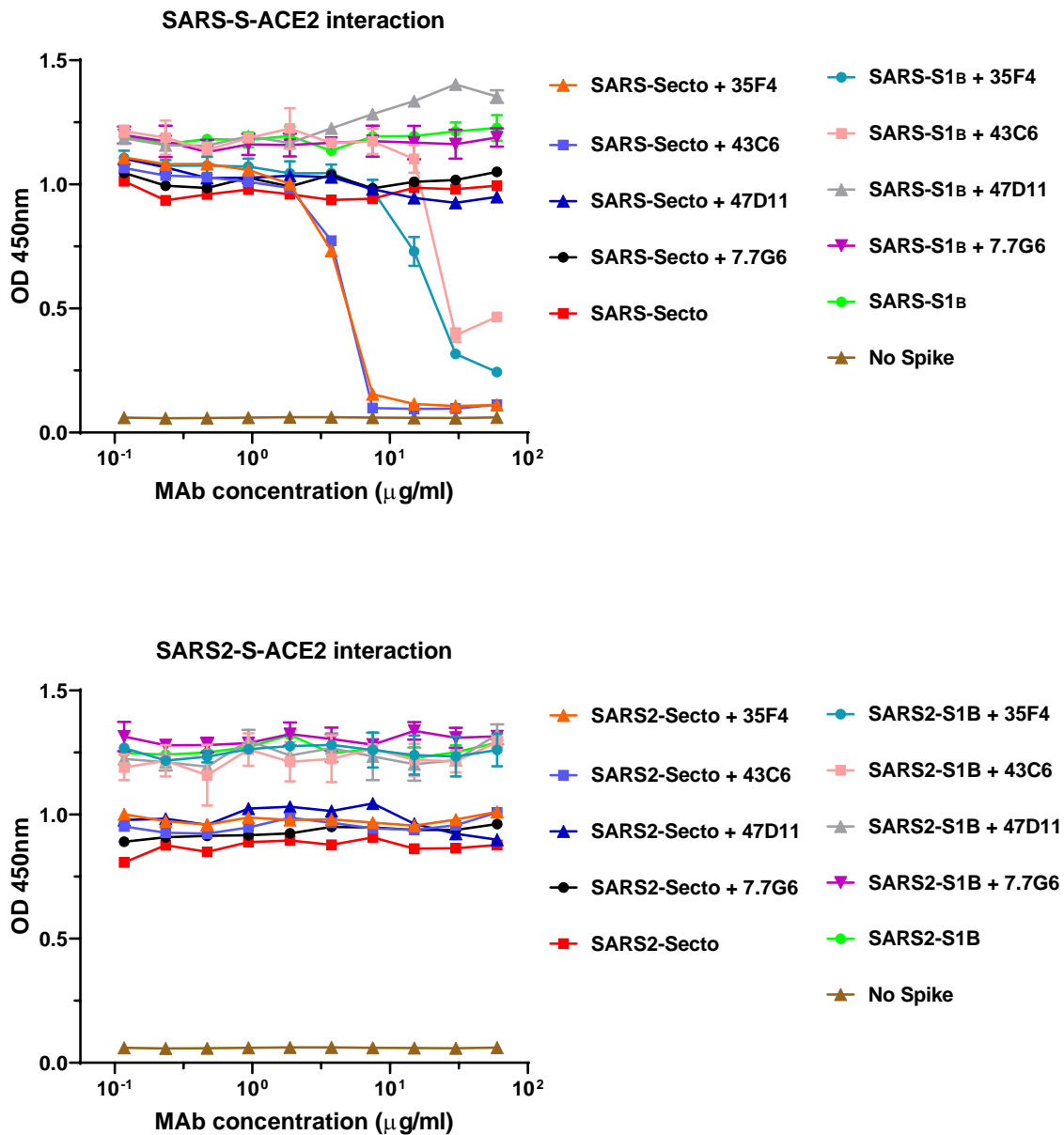


### Binding controls



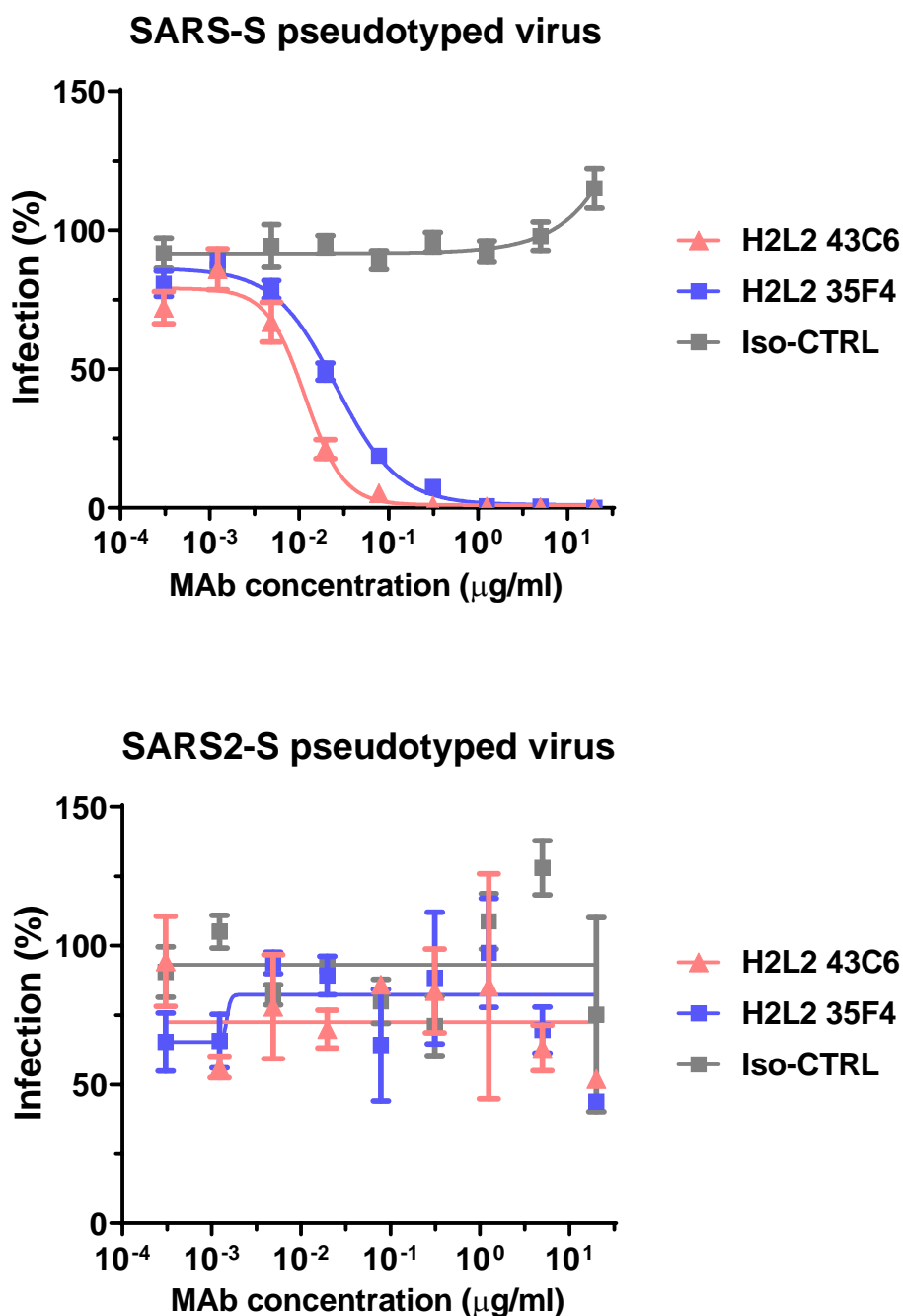
**SARS2-S1<sub>B</sub> – ACE2 receptor binding**

**Suppl. Fig.4. 47D11 does not prevent binding of SARS-S1<sub>B</sub> and SARS2-S1<sub>B</sub> to ACE2-expressing cells.** Human HEK-293T cells expressing human ACE2-GFP proteins (see Methods) were detached and fixed with 2% PFA, incubated with a fixed amount of human Fc-tagged S1<sub>B</sub> domain of SARS-S or SARS2-S that was preincubated for 1h with mAb (mAbs 47D11, 35F4, 43C6, 7.7G6, in H2L2 format) at the indicated mAb:S1<sub>B</sub> molar ratios, and analysed by flow cytometry using a Alexa Fluor 594-conjugated secondary antibody targeting the human Fc tag. Cells are analysed for GFP expression (x-axis, GFP signal) and antibody binding (y-axis, Alexa 594 signal). Percentages of cells that scored negative, single positive, or double positive are shown in each quadrant. Binding controls include PBS-treated cells (mock), treatment of cells with SARS-S1<sub>B</sub> and SARS2-S1<sub>B</sub> in the absence of antibody, and cells treated with antibodies only. The experiment was performed twice, data from a representative experiment are shown.



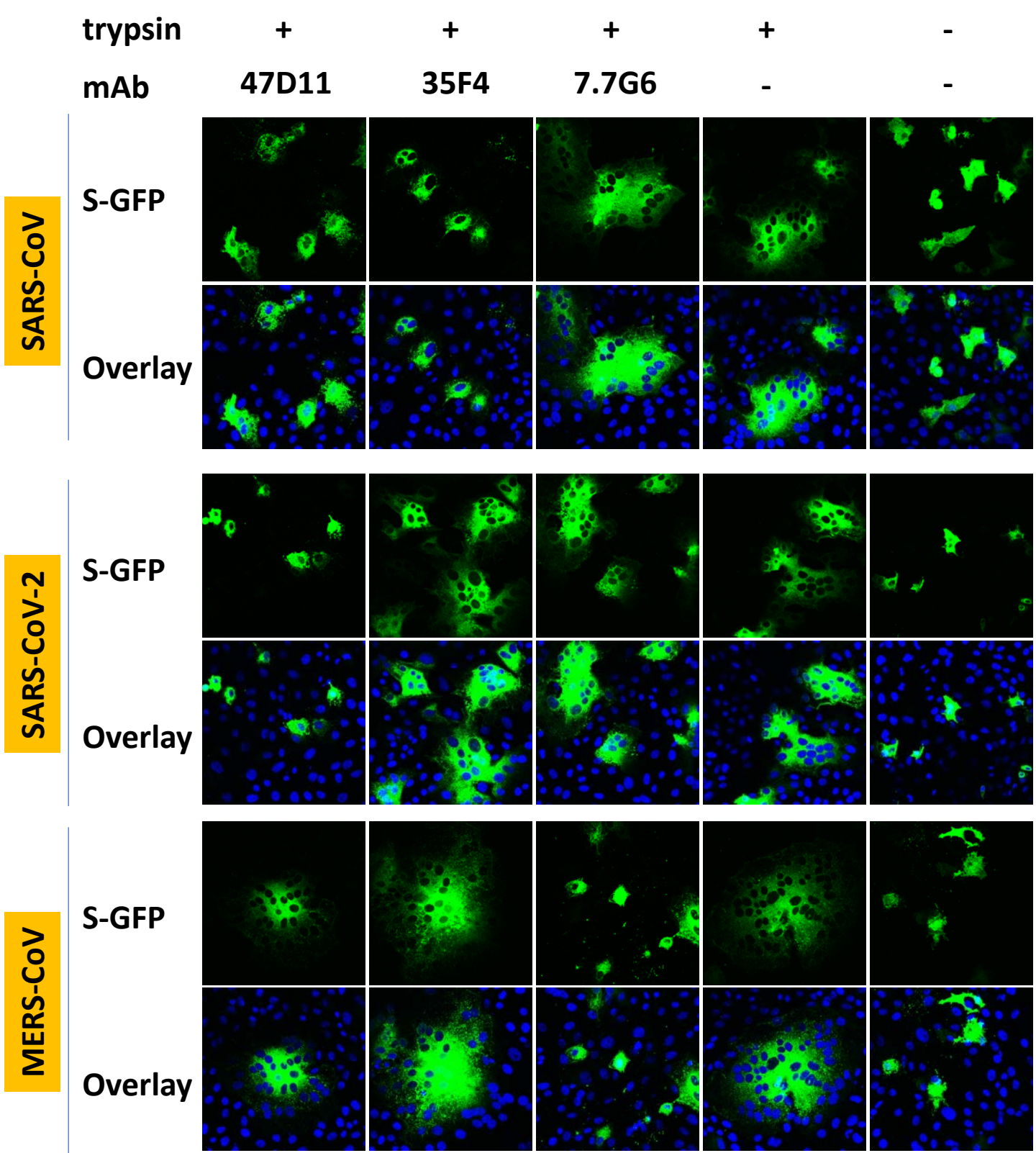
**Suppl. Fig.5. ELISA-based receptor binding inhibition assay.** The ELISA-based receptor binding inhibition assay was performed as described previously with some adaptations<sup>1</sup>. Recombinant soluble human ACE2 was coated on NUNC Maxisorp plates (Thermo Scientific) at 4°C overnight. Plates were washed three times with PBS containing 0.05% Tween-20 and blocked with 3% BSA in PBS containing 0.1% Tween-20 at room temperature for 2 hours. Recombinant S<sub>ecto</sub> and S1<sub>B</sub> of SARS-S or SARS2-S (300 ng) and serially diluted mAbs (mAbs 47D11, 35F4, 43C6, 7.7G6, in H2L2 format) were mixed for 1h at RT, added to the plate for 1 hour at room temperature, after which the plates were washed three times. Binding to ACE2 was detected using HRP-conjugated StrepMAb (IBA) that recognizes the C-terminal Streptag on the S<sub>ecto</sub> and S1<sub>B</sub> proteins.

1) Widjaja, I. et al. Towards a solution to MERS: protective human monoclonal antibodies targeting different domains and functions of the MERS-coronavirus spike glycoprotein. *Emerg. Microbes Infect.* 8, 516-530 (2019).



**Suppl. Fig.6.** H2L2 monoclonal antibodies 35F4 and 43C6 neutralize SARS-CoV but not SARS-CoV-2. Antibody-mediated neutralization of infection of VSV particles pseudotyped with spike proteins of SARS-CoV (upper panel) and SARS-CoV-2 (lower panel) by the 35F4 and 43C6 H2L2 antibodies targeting SARS-S1 but not SARS2-S1 (see Suppl.Fig.1). An irrelevant antibody was taken along as a human IgG1 isotype control. Means  $\pm$  SD of triplicates are shown.







**Suppl. Fig.7. Cell-cell fusion inhibition assay.** The cell-cell-fusion inhibition assay was performed as described previously with some adaptations<sup>1</sup>. VeroE6 cells were seeded with density of  $10^5$  cells per ml. After reaching 70~80% confluency, cells were transfected with plasmids encoding full length SARS-S, SARS2-S and MERS-S – C-terminally fused to GFP - using Lipofectamine 2000 (Invitrogen). The furin recognition site in the SARS2-S was mutated (R<sup>682</sup>RAR to A<sup>682</sup>AAR) to inhibit cleavage of the protein by endogenous furin and allow trypsin-induced syncytia formation. Two days post transfection, cells were pretreated DMEM only or DMEM with 20 µg/ml mAbs for 1 h and subsequently treated with DMEM with 15 µg/ml trypsin (to activate the spike fusion function) in the absence or presence of 20 µg/ml mAbs (47D11 crossreactive SARS-S and SARS2-S, 35F4 reactive to SARS-S, 7.7G6 reactive to MERS-S). After incubation at 37°C for 2 hrs, the cells were fixed with 2% PFA in PBS for 20 min at room temperature and stained for nuclei with 4,6-diamidino-2-phenylindole (DAPI). Cells expressing the S-GFP proteins were detected by fluorescence microscopy and S-mediated cell-cell fusion was observed by the formation of (fluorescent) multi-nucleated syncytia. The fluorescence images were recorded using a Leica Spell confocal microscope. The experiment was performed twice, data from a representative experiment are shown.

1) Widjaja, I. et al. Towards a solution to MERS: protective human monoclonal antibodies targeting different domains and functions of the MERS-coronavirus spike glycoprotein. *Emerg. Microbes Infect.* 8, 516-530 (2019).

# Suppl.Fig.8

```

SARS-RBD    323  CPFGEVFNATKFPSVYAWERKKISNCVADYSVLYNSTFFSTFKCYGVSATKLNLDLCSNV
SARS2-RBD   438  CPFGEVFNATRFASVYAWNRRKISNCVADYSVLYNSASFSTFKCYGVSPTKLNLDLCFTNV
          *****:* *****:**:*****:*****: ***** *****:**
SARS-RBD    383  YADSFVVKGDDVRQIAPGQTGVIADYNYKLPDDFMGCVLAWNTRNIDATSTGNINYKYRY
SARS2-RBD   396  YADSFVIRGDEVRQIAPGQTGKIADYNYKLPDDFTGCVIAWNSNNLDSKVGGNINYLYRL
          *****:***:***** ***** ***** **:***:.**:. ***** **
SARS-RBD    443  LRHGKLRPFFERDISNVPFSPDGKPCPT-PALNCYWPLNDYGFYTTTGIGYQPYRVVLSF
SARS2-RBD   456  FRKSNLKPFFERDISTEIYQAGSTPCNGVEGFNCYFPLQSYGFQPTNGVGYQPYRVVLSF
          *:.*:**:*****.  :.  ...**.  .:***:**:.***  *.*:*****
SARS-RBD    502  ELLNAPATVCGP
SARS2-RBD   516  ELLHAPATVCGP
          ***:*****

```

**Suppl. Fig.8. Protein sequence alignment of the S<sub>1B</sub> receptor binding domain (RBD) of the SARS-CoV and SARS-CoV-2 spike proteins by ClustalW.** Numbering denotes the residue position in the full-length spike protein of SARS-CoV (Genbank: AAP13441.1) and SARS-CoV-2 (Genbank: QHD43416.1). Asterisks (\*) indicated fully conserved residues, the colon symbol (:) indicates conservation between groups of very similar properties, and the period symbol (.) indicates conservation between groups of weakly similar properties. Sequences corresponding to the S<sub>1B</sub> receptor binding core domain and the receptor binding subdomain are colored in blue and orange, respectively. The fourteen residues that are involved in binding of SARS-CoV S<sub>1B</sub> to human ACE2 are highlighted in grey<sup>1</sup>.

1) Li, F., Li, W., Farzan, M. & Harrison, S. C. Structure of SARS coronavirus spike receptor-binding domain complexed with receptor. *Science* **309**, 1864-1868 (2005).